The Journal of Neuroscience, April 1994, 14(4): 2339-2356

Spatial Correlates of Firing Patterns of Single Cells in the Subiculum of the Freely Moving Rat

Patricia E. Sharp and Catherine Green

Department of Psychology, Yale University, New Haven, Connecticut 06520

Hippocampal lesions cause spatial learning deficits, and single hippocampal cells show location-specific firing patterns, known as place fields. This suggests the hippocampus plays a critical role in navigation by providing an ongoing indication of the animal's momentary spatial location. One question that has received little attention is how this locational signal is used by downstream brain regions to orchestrate actual navigational behavior. As a first step, we have examined the spatial firing correlates of cells in the dorsal subiculum as rats navigate in an open-field, pellet-searching task. The subiculum is one of the few major output zones for the hippocampus, and it, in turn, projects to numerous other brain areas, each thought to be involved in various learning and memory functions.

Most subicular cells showed a robust locational signal. The patterns observed were different from those in the hippocampus, however, in that cells tended to fire throughout much of the environment, but showed graded, location-related rate modulation, such that there were some localized regions of high firing and other regions with relatively low firing. There were slight quantitative differences between the proximal (adjacent to the hippocampus) and distal (farther from the hippocampus) subicular regions, with distal cells showing slightly higher average firing rates, spatial signaling, and firing field size. This was of interest since these two regions have different efferent connections.

Examination of spike trains allowed classification of cells into bursting, nonbursting, and theta (putative interneuron) categories, and this is similar to subicular cell types identified *in vitro*. Interestingly, the bursting and nonbursting types did not differ detectably in spatial firing properties, suggesting that differences in intrinsic membrane properties do not necessitate differences in coding of environmental inputs.

The results suggest that the subiculum transmits a robust, highly distributed spatial signal to each of its projection areas, and that this signal is transmitted in both a bursting and nonbursting mode.

[Key words: subiculum, hippocampal formation, place cells, spatial learning, bursting cells, nonbursting cells, theta cells, spatial information processing]

The hippocampal formation is thought to be critically involved in spatial learning. Lesions of this structure, or its major connections, cause learning impairments on a wide variety of navigational tasks (O'Keefe et al., 1975; O'Keefe and Nadel, 1978; Olton et al., 1978; Morris et al., 1982; Sutherland et al., 1983; Taube et al., 1992). In addition, physiological studies have shown that individual cells in this area have strong spatial firing correlates. In particular, cells in the hippocampus itself show location-specific firing patterns, such that any one cell is active only when the animal is in a circumscribed area of a larger environment (O'Keefe and Dostrovsky, 1971; O'Keefe, 1976; McNaughton et al., 1983; Muller et al., 1987). Each of these place cells has its own preferred location, such that, as a population, the hippocampal cells appear to provide an ongoing representation of the animal's momentary location in space. This finding is compatible with the fact that hippocampal lesions result in spatial deficits, since it seems likely that information about present location would be essential to many navigational abilities.

One question that has received little attention, however, is how this information is actually utilized to guide spatial behaviors. Thus, it is not clear to which brain regions the information is projected, or how it interacts with the circuitry in these areas in order to help orchestrate appropriate spatial trajectories.

One area that is critical for beginning to understand this question is the subiculum. The subiculum is a cortical region located adjacent to the hippocampal CA1 layer throughout much of its extent, and it receives a massive excitatory projection from these hippocampal cells (Andersen et al., 1973; Hjorth-Simonsen, 1973; Swanson et al., 1978; Finch and Babb, 1980, 1981; Amaral et al., 1991). It is, in fact, one of the few extrahippocampal projection sites for hippocampal pyramidal cells (Swanson and Cowan, 1975, 1977; Meibach and Siegel, 1977a,b), and it, in turn, projects to numerous other brain regions that are, themselves, each thought to be critical for particular learning and memory functions (Chronister et al., 1975; Meibach and Siegel, 1975, 1977a,c; Swanson and Cowan, 1975, 1977; Rosene and Van Hoesen, 1977; Sorensen and Shipley, 1979; Witter et al., 1990). Thus, the major projection areas for the subiculum include the nucleus accumbens, which is thought to be involved in instrumental learning (see, e.g., Fibiger and Phillips, 1988), the prefrontal cortex, which is thought to be involved in representational or working memory (see, e.g., Goldman-Rakic, 1987), the anterior thalamic nuclei and posterior cingulate cortex, which are thought to play a role in discriminative avoidance learning (see Gabriel, 1990), the perirhinal cortex, which is thought to be involved in visual and tactual memory (Zola-

Received July 26, 1993; accepted Oct. 4, 1993.

This work was supported by NSF Grant 9120131 to P.E.S.

Correspondence should be addressed to Patricia E. Sharp, Department of Psychology, P.O. Box 11A, Yale Station, Yale University, New Haven, CT 06520.

Morgan et al., 1989, 1993; Suzuki et al., 1993), and the entorhinal and postsubicular areas, which are, like the hippocampus, involved in spatial learning (Schenk and Morris, 1985; Taube et al., 1992). It seems possible, then, that the locational information available in the hippocampus is transmitted, via the subiculum, to these other brain regions, so that place information is incorporated into each of the various kinds of learning orchestrated in these areas.

To test this possibility, and to examine the exact nature of any spatial signal projected from the subiculum, we have examined the activity of individual cells in the dorsal portions of the subiculum as animals navigate in an environment. Our results complement those of an earlier study (Barnes et al., 1990), which has reported a highly distributed but reliable spatial signal for cells in subiculum, as recorded while animals performed on an eight-arm maze. Here, we use an open-field paradigm developed by Muller et al. (1987), which permits a spatially continuous monitoring of cell firing throughout the extent of the environment (since trajectories are not restricted to maze arms). Like the eight-arm maze, this environment has been utilized in several studies of hippocampal cell activity, so that any spatial patterns observed in the subiculum can be compared to those seen in the hippocampus, and insight can be gained into any transformation of the information that may take place as the hippocampal signal is projected onto the subicular circuitry. As an additional basis for comparison between subicular cells and hippocampal place cells, a few of the cells were examined under conditions in which the standard recording environment was altered somewhat, either by changing the location of a salient cue, or by placing the animal in an environment with a different geometry. These manipulations were similar to some of those that have been conducted for hippocampal place cells (Muller and Kubie, 1987).

In addition to looking for possible location-related correlates, it was also of interest to determine whether there were directional components in the subicular signal. In another portion of the subicular complex, known as the postsubiculum, cells fire as a function of the animal's head direction (Taube et al., 1990a,b). Each cell has an approximately 90° range over which it is active, so it fires rapidly whenever the animal's head is oriented in a direction (relative to the surrounding environment) within that range. Cells in the hippocampus also sometimes have a directional component (e.g., McNaughton et al., 1983), although, in the paradigm used here, this is typically very minimal compared to that for the postsubicular cells (Bostock et al., 1988). Since the subiculum is in a position to receive postsubicular information indirectly, via the entorhinal cortex (Steward, 1976; van Groen and Wyss, 1990), it was of interest to know the extent to which a directional component would be evident in the subicular signal.

One additional question of interest was based on the finding that the subiculum is heterogeneous across its transverse extent in terms of its projection areas (Witter et al., 1990). Cells in the distal portions of the dorsal subiculum (that part farthest from the hippocampus) project to a set of areas that includes the retrosplenial cortex, presubiculum, anterior thalamic complex, and caudal mammillary nucleus, while cells in the proximal portion (closest to the hippocampus) project to the entorhinal and perirhinal cortices, infralimbic cortex (a part of rat prefrontal cortex), rostral mammillary nucleus, nucleus accumbens, and lateral septal area. Thus, it was of interest to see whether there might be any differences in the nature of the spatial signal sent to these two sets of areas. Because of this, an attempt was made to sample cells throughout the transverse extent of the subiculum.

Also of interest was whether there would be any evidence for subtypes of spatial firing correlates for cells within each local portion of the subiculum. One finding that suggested this possibility was the fact that different subicular cells within any local area are somewhat specialized in their efferent connections, such that any one cell projects to only a subset of all the projection areas for that part of subiculum, and two adjacent cells are likely to have two different subsets (Swanson et al., 1981; Donovan and Wyss, 1983). Thus, it seemed possible that these different projection patterns could correspond to cells with different behavioral correlates.

Another suggestion that there could be subtypes came from a recent *in vitro* study by Stewart and Wong (1993), which showed that the subicular projection cells could be divided into bursting (named after their ability to fire a burst discharge to direct depolarization, as well as either antidromic or orthodromic stimulation), nonbursting, and interneuron types. At least a portion of the burst response for bursting cells was Ca^{2+} dependent, and bursts were followed by a brief afterhyperpolarization. Sustained depolarization could cause the bursting cells to enter a single-spike mode. It was of interest to know whether these different firing patterns would also be present in an *in vivo* situation, where the cells are functioning in the context of the complete brain circuitry. In addition, it seemed possible that this difference in physiological cell type could lead to differences in spatial firing correlates. Thus, for example, it could be that the depolarizing envelope provided by a bursting pattern might facilitate a long-term potentiation (LTP)-like process with regard to hippocampal place cell inputs. Such LTP could, conceivably, result in a more robust spatial signal. Alternatively, it could be imagined that the intrinsic rhythmicity imposed by the bursting cell physiology could cause a less strong spatial signal, since this rhythmicity would not likely be in phase with the animals' transitions into and out of preferred firing regions. Thus, in general, the presence of these two cell types in the same cell layer provided an opportunity to see how cells that differ in underlying physiological properties might process the same set of afferent inputs (although it cannot be assumed that the details of hippocampal–subicular connectivity are identical for the two types).

In addition to these two types of projection cell, Stewart and Wong also identified a third cell type that had a shorter spike width than cells in the above two categories and fit the general profile of inhibitory interneurons that have been identified in CA1. In the hippocampus, interneurons like these have been identified as theta cells (Ranck, 1973; Fox and Ranck, 1975), which, in an *in vivo* situation, show high firing rates, fire most rapidly when the hippocampal theta EEG pattern is present, and fire in phase with this theta rhythm, when present. It was of interest to see whether a similar cell type could be identified in the subiculum.

Autocorrelation functions of subicular spike trains in freely moving animals exhibit a wide spectrum of patterns (Barnes et al., 1990), and this is compatible with the idea that there could, in fact, be bursting, nonbursting, and theta cell types. Here, both autocorrelation and interspike interval histograms have been used to examine spike train patterns.

One final question was whether or not the subicular cells would show any evidence of a columnar pattern of organization,

such that cells close together, or along the same vertical trajectory, would show similar spatial correlates. This possibility was suggested by recent anatomical data showing a topographical organization for the hippocampo-subicular projection (Amaral et al., 1991), and that individual hippocampal cells terminate in a columnar, or slab-like fashion in the subicular cell layer (Tamamaki et al., 1987; Tamamaki and Noyjo, 1990). Thus, it could be that adjacent subicular cells receive sufficiently similar hippocampal inputs that they would show similar coding of location.

Materials and Methods

Experimental subjects

The subjects were 21 female Long–Evans rats, weighing 200–250 gm at shipping. Animals were housed singly upon arrival, and had a 12 hr on (8:00 A.M. to 8:00 P.M.)/off, light/dark schedule.

Apparati

The standard recording chamber was a 76-cm-diameter, 51-cm-high, cylindrical chamber (Muller et al., 1987). The inner wall was painted uniformly gray, and was equipped with a single white card, which extended from the floor to the top of the cylinder wall, and covered 100° of arc. The chamber had no floor, but was laid on replaceable, gray photo-backdrop paper. The entire cylinder was surrounded by a uniform, circular curtain that formed an enclosure 175 cm high and 137 cm in diameter at its widest, and then tapered off above this to a diameter of 57 cm, and a height of 213 cm. Illumination was provided by a single 100 W overhead light (located in an inverted position above the curtain), which spread a diffuse, uniform light over the cylinder floor. Also located above the curtain was an automatic dispenser for the remote-controlled delivery of food pellets. Pellets dispensed in this way dropped to a position near the center of the cylinder floor and scattered to random locations throughout the area of the cylinder. The cylinder was located in a room separate from the recording equipment.

For some sessions, a 39-cm-wide, 55.5-cm-long, 51-cm-high rectangular apparatus was used, and it was also placed inside the circular curtains, when in use. In addition, it was similarly painted uniformly gray, and equipped with a single white card that extended from the floor to the top of one end wall.

Behavioral training

Prior to training, rats were placed on a food deprivation schedule in which they were reduced to 80% of their ad libitum weight through limited daily feeding. They were then trained to search for 20 mg food pellets (BioServe, Frenchtown, NJ) that were thrown into the cylinder at pseudorandom locations, at approximately 15 sec intervals. During training, the cylinder was located in a separate room from the one in which cell screening and recording were later conducted. To begin each daily 15 min training session, each rat was placed into the cylinder at a fixed angular location (90° clockwise to the center of the white card), which was the same as that used in the later "standard" recording sessions (see below). A total of six training sessions were given; for the first three sessions animals chased pellets in the chamber in groups of two or three, while the last three were administered individually. During this period, rats developed a pattern of nearly constant locomotion that lasted throughout the sessions and resulted in the rat covering the entire cylinder floor repeatedly throughout the session, in an apparently homogeneous fashion.

Electrode implantation

After training, two driveable microrecording electrodes (one per hemisphere), consisting of six wires each, were chronically implanted. The six separate wires, cut at an approximately 45° angle, consisted of Formvar-insulated, 25-μm-diameter, nichrome wire (California Fine Wire Co., Grover City, CA). Prior to surgery, animals were anesthetized with a 0.18 cc injection of 65 mg/ml pentobarbital, and supplemental doses were given during surgery, if necessary, to maintain deep surgical anesthesia. The rat was placed in a Kopf stereotaxic frame, the skull was exposed, and three securing screws were placed in the skull over each of the frontal and cerebellar cortices. An approximately 2 mm hole was drilled in the scull over the dorsal subiculum of each hemisphere to allow electrode insertion. To sample cells throughout the extent of the dorsal subiculum, electrode placements were varied through a range of 6.04–6.30 mm posterior, and 2.90–3.20 mm lateral to bregma. In most cases, a different pair of coordinates was used for the two hemispheres of each rat in an attempt to get two different subicular locations within the each rat. At surgery, the electrodes were placed 2.0 mm below the brain surface, so that their tips were well above the subicular cell layer, and could be gradually lowered through this layer after recovery. Sterile petroleum jelly was applied to the exposed brain surface, as well as the guide cannula surrounding the recording wires. The electrodes and securing screws were then cemented permanently to the scull by dental acrylic (Turotech, Wynnewood, PA). One of the securing screws was equipped with a connecting pin that protruded out from the dental acrylic so that it could be used as a grounding wire during recording. Also cemented into the acrylic was a small connector, used for later attachment of the recording equipment.

Unit isolation and data collection

After recovery from surgery, the activity from each electrode wire was sampled one or more times each day, while the rat performed the pellet-retrieving task in the cylinder. The electrode tips were gradually lowered through the cell layer, over a period of several weeks, so that the activity of single subicular cells along the electrode track could be isolated. Two wires could be recorded from at the same time, and the signal from each was passed first through a field-effect transistor in source-follower configuration that was mounted on the pin attached to each electrode wire. This signal then passed through a cable (affixed to the connector on the animal's head) to an amplifier (10,000 gain) and filter (300 Hz high pass, and 10 kHz low pass), and then to a computer, for automatic data collection. The software used for data collection and cell discrimination (Brainwave Corporation) collected an epoch of the digitized analog signal for every event from the amplifier that exceeded a user-set threshold. These events were then separated into bins, each of which captured the waveforms generated by spikes from one individual cell, through a cluster analysis routine that utilized information from eight different parameters extracted from each waveform. In this way, it was often possible to collect data from more than one cell simultaneously. Each event, along with a time stamp and indication of which bin it belonged to, was automatically stored.

The animal's moment-to-moment position in the cylinder was also sampled continuously throughout each session. For this, a video camera located above the cylinder monitored the location of two light-emitting diodes attached to the animal's head. One of these lights was toward the front, while the other was toward the back of the animal's head. The video signal was sent to a camera tracking system (Brainwave Corporation) that extracted a digitized representation of the location of each of the two lights for transmission to the computer at a rate of 60 Hz. This information was time-stamped and automatically stored. The fact that there were two headlights made it possible to calculate later not only the momentary location of the animal's head (taken as the midpoint of a line drawn between the two lights) but also the direction in which the animal's head was pointing.

Testing paradigm

Upon isolation of appropriate single-cell activity, a "standard" recording session, lasting between 20 and 40 min, was conducted. For these sessions (as well as all screening sessions), the cue card was located in the 3:00 o'clock position (relative to the video camera framework). The animal was carried to and from all screening and recording sessions in a covered, opaque cage (the top of which was removed only after entering the circular curtains), and the animal was introduced into the cylinder by being placed next to the wall at 6:00 o'clock. Pellets were delivered from the overhead dispenser at variable intervals (with an average of approximately 20 sec) throughout the session. Animals typically engaged in constant locomotor activity, repeatedly covering each portion of the cylinder floor, through a variety of different trajectories, many times over the session. The experimenter always entered and left the curtained area from the 6:00 o'clock position.

For some cells, more than one standard session was conducted. These repeated sessions were not planned, but happened sometimes because the initial session was interrupted due to technical problems. Other times, repeat sessions were conducted if a cell remained present on a wire for more than 1 d.

For eight of the cells, a series of three additional sessions was con-

ducted after the initial standard session, in order to provide a preliminary investigation of some of the environmental influences on these cells. For this, both the cylinder and the rectangle were placed inside the circular curtain (see Fig. 8), with the rectangle adjacent to the cylinder (which was slightly displaced downward from its usual position, so that both apparati could fit within the camera field). The cylinder was rotated so that the card was at 12:00 o'clock while the card in the rectangle was at 9:00 o'clock. The first session of the series (lasting 15–20 min) took place in the cylinder, and the animal was introduced to this at the 3:00 o'clock position. Note, this means that the angular relationship between the card and the entry location was the same as for standard sessions. Thus, this session enabled a test of whether these two variables together could determine the orientation of the spatial firing patterns. Since these were the only two orienting cues that were intentionally provided, this session served as a test for the influence of any uncontrolled background cues.

For the next session (15–20 min in duration), the animal was transferred directly from the rotated cylinder to the rectangle. This enabled a determination of whether a cell would have a field in more than one environment, as well as a test of similarities in firing in the two environments. The fact that this environment also had a white card, but the card was in a different angular location, provided a test of whether the card itself, now in a new context, would cause similar effects to those in the cylinder.

For the final session (15–20 min), the cylinder was rotated back to the standard angular position (this was done while the animal was performing the pellet-retrieving task in the rectangle) and the animal was then transferred directly back into the cylinder. This manipulation allowed a test of the relative influence of the card and entry angle in the context of the cylinder, since they were now out of their usual angular relationship to each other.

Data presentation and analysis

Firing rate maps. In order to visualize any location-related firing patterns, the time of occurrence for the spikes of a given cell, along with the position data, were used to construct a firing rate map for each cell (Muller et al., 1987). For this, the cylinder was divided into 2.9 by 2.9 cm pixels, and the total amount of time spent in each pixel, along with the total number of spikes that occurred when the animal was in that pixel, were used to calculate an average rate for each. The relative rate in each was indicated in the map using a gray scale, the value of which was chosen based on the mean and standard deviation of the pixel rates for that cell (see Fig. 2 for details). A diagonal line was used to indicate pixels that the animal visited, but in which the cell did not fire. A blank pixel means that the animal did not visit that location during the session.

Direction-specific firing rate maps. In order to visualize any direction-related firing properties, a circular array of maps (Taube et al., 1990a; see Fig. 4) was constructed, each of which showed firing rate for only those samples taken when the animal was facing the direction indicated by the accompanying arrow (actually, each arrow indicates the center of a 45° directional range). Gray-scale values for all maps are based on the mean and standard deviation for values in the central map (constructed as described above). Thus, darker pixels in a particular direction-specific map indicate higher rates when the animal was faced in that direction.

Rate. The overall rate (in hertz) for each cell was calculated by dividing the total number of spikes in the session by the total session time (in seconds).

Rate in nonzero pixels. In addition to the above rate measure, it was also necessary to calculate the average rate for the nonzero cylinder pixels. This was necessary since many of the cells did not fire everywhere in the cylinder, but rather, only within a circumscribed area(s). This meant that the overall rate would be affected by the size of this active area. It was useful, however, to be able to compare cell rates for only those regions that were contained within each cell's field.

Field size. The size of the firing field for a given cell was calculated as the percentage of visited pixels in which the rate was above zero.

Spatial coherence. This measure provides one way of quantifying the strength of the spatial signal for a cell, and is very similar to the spatial coherence measure developed by Kubie et al. (1990). It consists of a spatial autocorrelation, in which a correlation coefficient is calculated between the rate for each pixel, and the average rate of the eight surrounding pixels. Thus, high, positive values for R result if the rate for each pixel can be better predicted by knowing the rate of the neighboring pixels. This means the R value serves as a measure of any consistent, graded, location-related variations in rate.

One possible problem with using the average pixel rate values (as were used for firing rate map construction) for calculating this statistic arises from the fact that some cells were also influenced by directional heading. Because of this, an overestimate of the strength of the spatial signal could result from any nonorthogonality in the animal's behavior between locational position and associated directional heading. Thus, imagine a case in which a cell has a strong directional component, such that it fires most rapidly when the animal is facing north. Since it is not possible for the animal to face north when its head is located along the far southern edge of the cylinder (the animal's body prevents this possibility), this would cause a region of relatively low firing in this southern portion of the cylinder, and would contribute to a high, positive R value. This low firing zone would be caused, however, not by a true locational bias for the cell, but by a directional bias in combination with mechanical restrictions on what directions are obtainable in certain locations. Similarly, there might be other regions of the cylinder (such as those portions of the cylinder edge that are roughly parallel to the north–south axis) that would show relatively high rates, due to the fact that the animal may spend proportionally more time facing north in those locations.

To control for this possible direction-related confound, pixel rates for the spatial coherence measure were first corrected for this influence. For this, a corrected rate for each pixel in each of the direction-specific bins described above (for the construction of direction-specific firing rate maps) was obtained by subtracting the average rate of pixels across all locations in that direction-specific bin from the rate for that particular pixel. Thus, if the rate for a given pixel in that bin is higher than the average rate for those direction-specific pixels, the number will be positive; if it is lower than the average rate for that direction, it will be negative. Finally, the pixel rate value actually used for the spatial coherence calculation was obtained by taking the average of these corrected, direction-specific values. Thus, the logic used here is similar to that used in the analysis of covariance, in which the predicted value based on the estimated influence of a covariate is first subtracted from the obtained value. In this way, significant values for spatial coherence could be obtained only if location has an influence beyond that which could be predicted by the influence of directional heading.

Quantitative analysis of directional influences. To assess the statistical significance of any directional component of the cell activity, an analysis of variance was conducted for the pixel rates in the set of direction-specific bins described above (using bin membership as the independent variable). These values were first corrected, however, to remove possible confounding influences due to location-related rate variations. Thus, again due to the nonorthogonality of locational and directional aspects of the rats' behavior, it was possible that location-related variance in firing rate could cause apparent directional effects. As an example, imagine a cell that had a high firing rate along the south wall of the cylinder (a locational correlate). Since the animal cannot face north when its head is close to this wall, this would artifactually result in lower average firing in the north-specific bin. To correct for this, the average rate (computed across all sampled directions) for each pixel was subtracted from each direction-specific rate, to yield direction-specific values from which location-related effects had been removed.

In addition to an F value to assess the statistical significance of any directional effects, an ω^2 value was also calculated. This statistic provided a measure of the proportion of total variance that could be accounted for by directional heading.

Spike train analysis. Temporal patterns in the spike trains were examined through two types of histogram. Interspike interval histograms were constructed by summing the number of occurrences of intervals between successive spikes that fell within each 1 msec time bin from 0 to 300. The sum of each bin was then divided by the total number of interspike intervals, in order to obtain the proportion of interspike intervals that fell within each 1 msec time range. Any tendency for a cell to fire in bursts at a given frequency will show up as a peak at the corresponding interval in the interspike interval histogram.

Autocorrelation histograms were constructed by summing the number of times in which a spike occurred within each 1 msec bin from 0 to 300, given the occurrence of a spike at time 0. These sums were then divided by the total time, to yield the rate of occurrence for each interval. These histograms reveal any rhythmic modulation of cell rate, and also provide an indication (based on the average height of the histogram bars) of the overall firing rate.

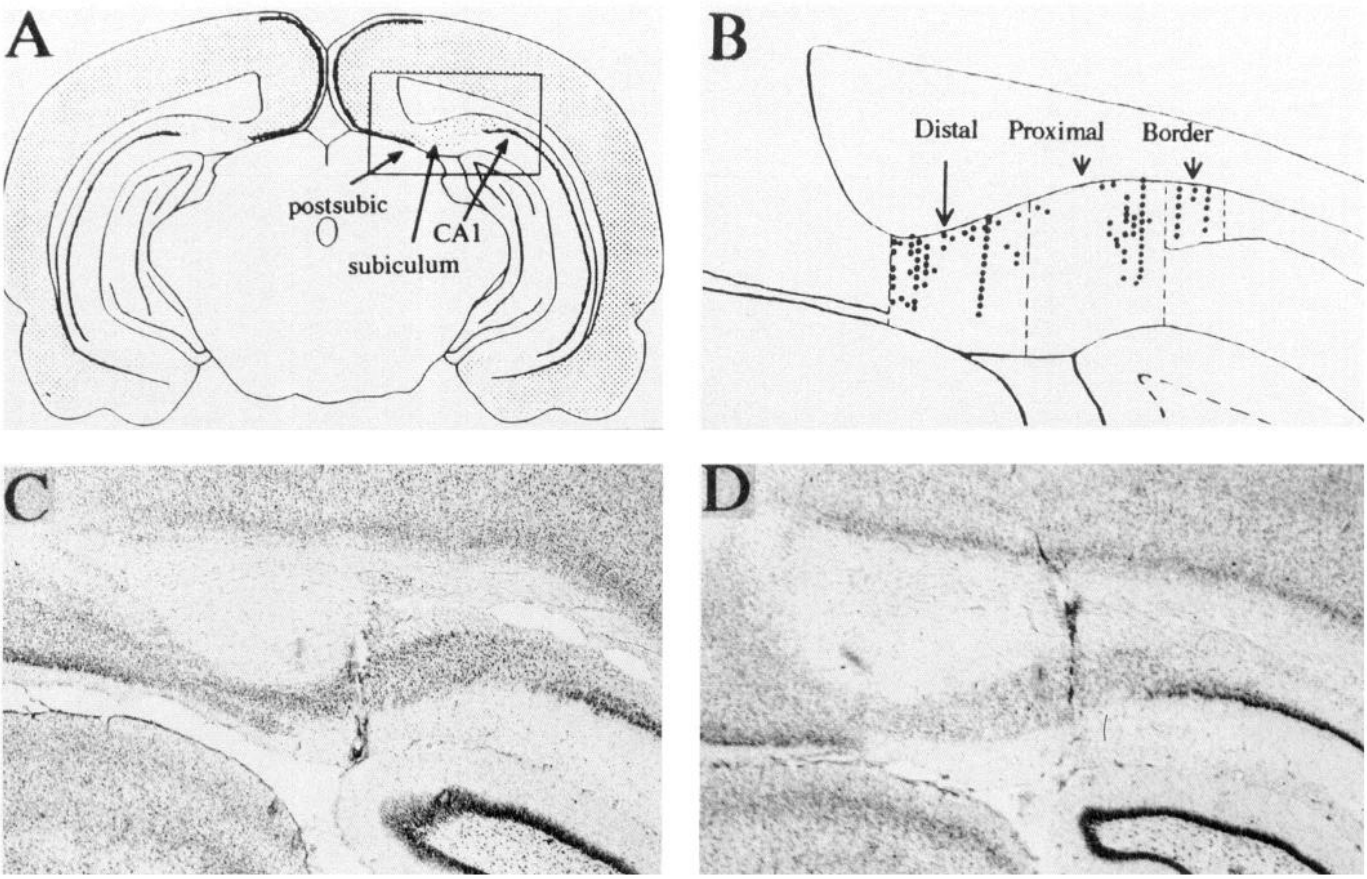

Figure 1. Summary illustration of histological findings. *A,* Coronal section through the rat brain at a level 6.04 posterior to bregma. *B,* Composite drawing of the estimated location of each of the cells included in the data set. Also shown are the lines according to which the subiculum was divided into sections for subsequent analysis. The hippocampo-subicular border region is a zone in which both a hippocampal pyramidal cell layer is present, as well as an overlying, less dense, subicular cell layer. The line dividing the subiculum itself into sections is not based on anatomical criteria, but simply divides the subiculum into equal halves. *C* and *D,* Examples of electrode tracks through the distal and proximal regions, respectively, of dorsal subiculum.

Correlations between firing rate maps. Similarity between pairs of maps (such as maps resulting from repeated sessions on the same cell) was assessed by calculating a pixel-by-pixel correlation coefficient between the two.

Histological examination and reconstruction of cell location

After recording, animals were perfused transcardially under deep anesthesia with a formyl saline solution. Prior to this, a small current (30 μA × 5 sec) was passed through one wire of each electrode, in order to mark the location of the electrode tips. The brains were then sectioned in the coronal plane at 40 μm intervals, mounted, and stained with both cresyl violet and Prussian blue.

Microscopic examination revealed the transverse location of the electrode track along which each cell was recorded. The dorsoventral location within the cell layer for each cell was estimated through examination of records kept during cell screening. This method utilized the fact that the subicular cell layer is surrounded both dorsally and ventrally by physiologically quiet zones, so that the presence of large multiple-unit activity provided a clear indication of when the electrode entered and then exited the cell layer as it was lowered over days (screening was typically continued until the electrode tips reached the ventrally located quiet zone). Thus, the approximate vertical location of each cell could be reconstructed.

These locations were drawn on a composite map (Fig. 1*B*), in which the transverse axis of the dorsal subiculum was divided into distal (relative to the hippocampus) and proximal halves, as well as a hippocampo-subicular border region. In this latter area, both a densely packed hippocampal cell layer, as well as a more dorsal, less dense layer (typical of the subicular cell layer) could be observed.

Results

Cell sample

Data were collected from a total of 99 cells in 28 hemispheres of 21 rats. Histological examination revealed that the cells were located throughout the transverse extent of the dorsal subiculum, as well as in the border region between the hippocampus and subiculum. Figure 1*A* shows a coronal section through the rat brain at a level approximately 6.04 mm posterior to bregma. A summary diagram of the locations of all cells recorded, along with an indication of how the subicular region was divided into sections, is shown in Figure 1*B*. Each dot corresponds to the location of one cell, and vertical rows of dots correspond to cells recorded along a single electrode track. It can be seen that recorded cells were reasonably well distributed along the transverse axis, although the more distal portion of the proximal half was, by chance, not well sampled. The largest number of cells recorded along any one track was 14, and this number was obtained in the case of two electrodes. Examples of electrode tracks located in a distal and proximal portion of the subiculum can be seen in Figure 1, *C* and *D,* respectively.

The average firing rate for all cells recorded during performance of the pellet-chasing task was 9.05 (±1.41) Hz. Most cells showed a triphasic waveform (negative-positive-negative),

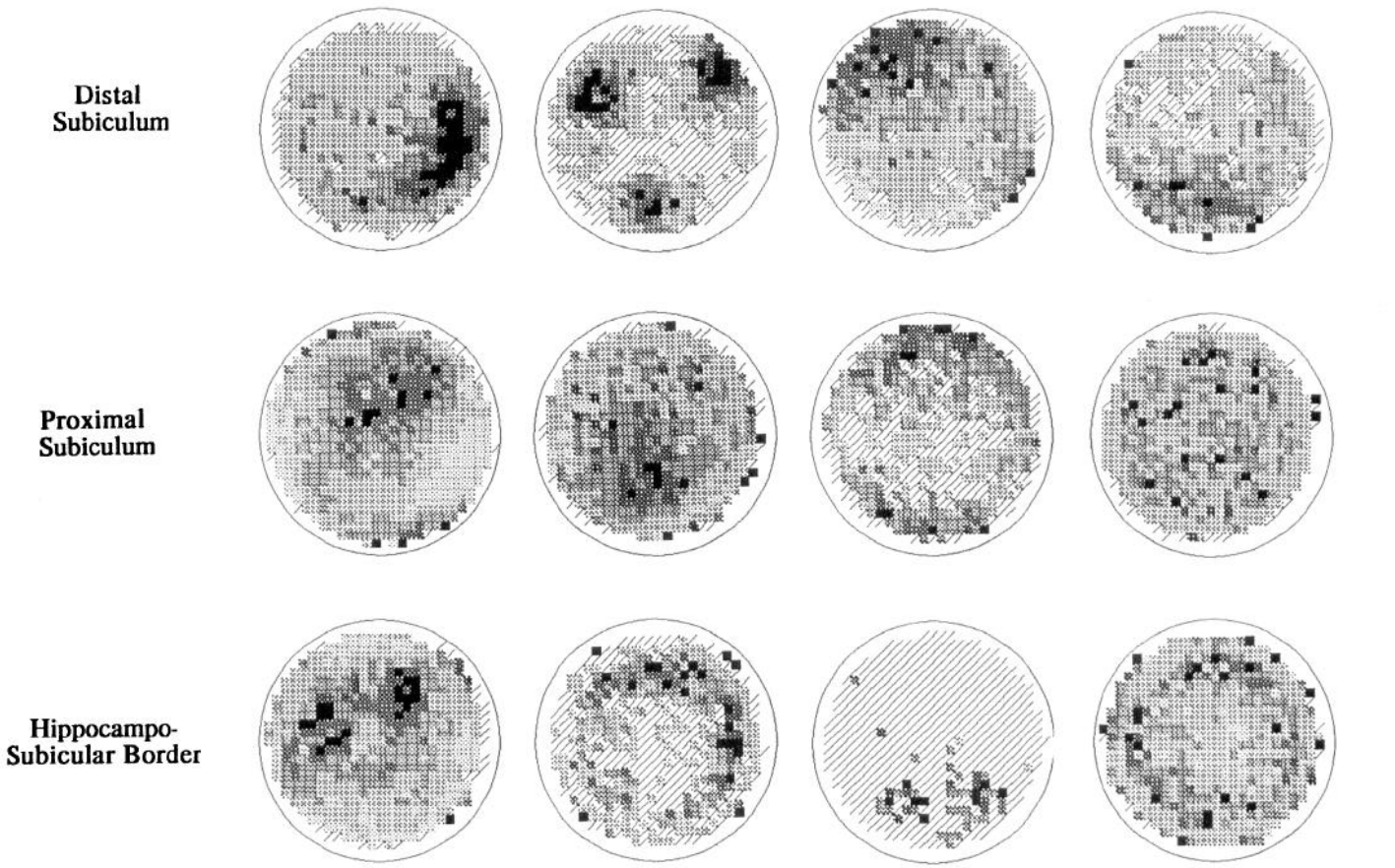

Figure 2. Location-related firing properties: firing rate maps for a set of 12 typical cells (four cells from each of the distal, proximal, and border regions) recorded from dorsal subiculum of 11 different animals during 20–40 min sessions. For map construction, the cylinder floor was divided into 2.9 cm by 2.9 cm pixels, and the firing rate for each pixel was obtained by dividing the total number of spikes that occurred when the rat was in that location by the total time spent in that location. These values were then used to compute a mean and SD over all the pixel rates. The relative rate for each pixel is depicted using one value of a five-valued gray scale so that pixels that are more than 2 SDs above the mean pixel rate for that cell are given the darkest value, those between 1 and 2 SDs above the mean have the next-highest value, those within 1 SD above the mean use the next value, those within 1 SD below the mean receive the next value, and those that are 1 or more SDs below receive the lowest value. Pixels that the animal visited, but in which the cell did not fire, are indicated by a *diagonal line. Blank pixels* indicate regions that were not visited during the session. Most cells fired throughout much of the area of the cylinder but showed consistent location-related modulation. Values for the mean (SD) for pixel rate of each map for each region, listed from left to right, are distal, 5.86 (5.86), 4.34 (7.52), 7.2 (6.04), 2.12 (3.98); proximal, 26.08 (11.17), 4.26 (2.14), 2.41 (4.17), 8.46 (8.21); border, 13.54 (10.29), 1.91 (3.76), 0.15 (0.90), 11.62 (5.07). Values for the spatial coherence measure for each map for each region, listed from left to right, are distal, 0.85, 0.84, 0.71, 0.29; proximal, 0.79, 0.47, 0.38, 0.19; border, 0.83, 0.46, 0.23, 0.20.

and for cells of this form, the average spike width, measured from the point of departure from baseline to return, was 331.78 (±18.98) μsec. The average amplitude from the initial negative to the subsequent positive peak was 369.55 (±29.57) μV.

Location-related firing properties

The majority of cells throughout the transverse extent of the dorsal subiculum showed strong location-related modulation of their firing rates. Eighty-three of the 99 cells showed significant ($p < 0.01$) R values for the spatial coherence measure, with the average R value for all cells being 0.48 (±0.02). The average R^2 value was 0.26, suggesting that (after removal of any directional component of the firing, as described in Materials and Methods) an average of 26% of the variance in firing rate could be accounted for by the momentary spatial location of the animal. The range of R values was from −0.04 to 0.92, and these values were scattered continuously throughout this range.

Figure 2 shows examples of firing rate maps for typical cells taken from each of the distal, proximal, and border regions of the dorsal subiculum. With the exception of the left two maps in the border region, each of the represented cells was recorded from a different animal. The firing rate maps for each region are arranged in order of spatial coherence, with the highest spatial coherence values located in the leftmost map for each region. It can be seen that the cells tended to fire throughout much of the area of the cylinder floor, while showing graded modulation of their rate as a function of location. Thus, each cell had one or more "hot spots" in which the firing rate was greater than average, as well as other regions in which it was consistently lower. The average field size (percentage of cylinder pixels in which the rate was above zero) for the subicular cells was 0.84, and this value confirmed the impression obtained during observation of the recording sessions that many cells seemed to fire continuously throughout the session.

These spatial firing patterns are quite different from the location-specific patterns typically observed for hippocampal place

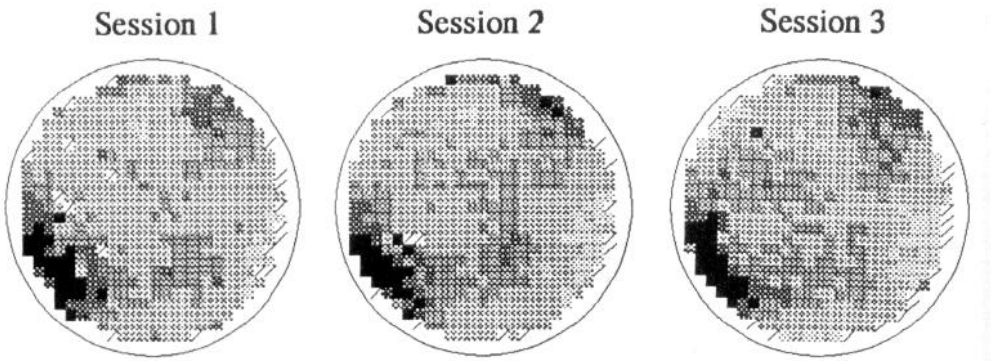

Figure 3. Stability of location-related correlates: firing rate maps (constructed as in Fig. 2) for three standard sessions conducted for the same cell. The first two sessions were 20 min long, while the last was 30 min. The location-specific pattern was highly repeatable.

cells. The hippocampal cells are typically silent throughout much of the enclosure, with a relatively small, unitary region of rapid firing in one location.

For cases in which data were obtained from the same cell over more than one session, locational firing patterns were quite stable across sessions. Figure 3 shows an example of a cell recorded from on three separate sessions, which took place over 2 d. The location-specific pattern was quite similar over repeated sessions. There were a total of seven cells for which more than one standard session was conducted, and the average pixel-by-pixel correlation coefficient for the rate maps of each initial and repeated session was 0.49 (±0.08). As a comparison, a correlation coefficient was also calculated for each of these same initial sessions and another map from the same electrode track, which was matched as closely as possible for rate. The average of these coefficients was −0.06 (±0.06), demonstrating that the correlation for the same cell over repeated sessions was much higher than for two different cells along one electrode track.

Direction-related firing properties

Many cells (60 of 98) showed a significant effect (df = 7,∞, $F > 2.64$, $p < 0.01$) of directional heading on firing rate. Figure 4 shows an example of a cell for which head direction had a relatively strong influence. Rates were relatively higher when the rat was facing any of the directions included roughly within the range represented by the maps in the lower half of the circular array. This cell also had a strong location-related signal (spatial coherence = 0.82), and this aspect of its signal appeared within each direction-specific map. Thus, the strength of the location-specific activity was modulated by directional heading.

Although many of the cells showed a significant influence of head direction, as assessed by ANOVA, examination of ω^2 values showed that for most cells only a very small proportion of the variance could be accounted for by this variable. The average of the ω^2 values was 0.01 (±0.002), with values ranging from 0.0 to 0.13, so even for the most strongly directional cell, only 13% of the variance could be explained by head direction. Thus, in general, head direction was a reliable but very small influence on firing rate, and for this reason, the influence of this variable will not be analyzed further.

Variation in firing properties related to anatomical location within subiculum

Table 1 shows mean values and SEs for firing rate, mean firing rate of nonzero pixels, spatial coherence, and field size for cells grouped according to anatomical location (as indicated in Fig. 1*B*). Values for all these measures were higher in the distal region of subiculum than in the proximal. Values in the border region were intermediate between these two for the rate measures, while they were lower than both of the other two regions for the spatial coherence and field size measures.

To assess the statistical significance of these regional differences, it was thought necessary first to obtain mean values of each of these measures for the cells recorded along each electrode track. In this way, it was possible to avoid sampling biases due to collection of numerous cells from a single electrode track, since data from each track contributed only one value to the ANOVA. Cells were collected from a total of 16 tracks in the distal region, nine in the proximal region, and three in the border area. Due to the small number in the border region, these cells were omitted from statistical analysis. *T* tests of the statistical significance of the differences between the distal and proximal areas yielded no significant differences on any of the measures shown in Table 1, although the tests for differences in spatial coherence and field size approached significant (df = 23; $t = 1.41$, $p < 0.20$, and $t = 1.27$, $p < 0.25$, respectively).

This lack of significant differences was surprising, given the apparently nontrivial differences in mean values for averages over individual cells (Table 1). In fact, *t* tests conducted using individual cells as data points (rather than hemisphere means)

Table 1. Averages of firing property measures for cells grouped according to anatomical location

Measure	Distal subiculum	Proximal subiculum	Hippocampo subicular border
Overall rate	11.16 (±1.77)	6.26 (±1.41)	8.23 (±3.46)
Mean rate for nonzero pixels	16.21 (±2.41)	9.01 (±1.97)	11.27 (±4.98)
Spatial coherence	0.59 (±0.03)	0.38 (±0.04)	0.30 (±0.06)
Field size	0.88 (±0.02)	0.78 (±0.04)	0.71 (±0.09)
N	52	34	13

Values are given as means (±SE).

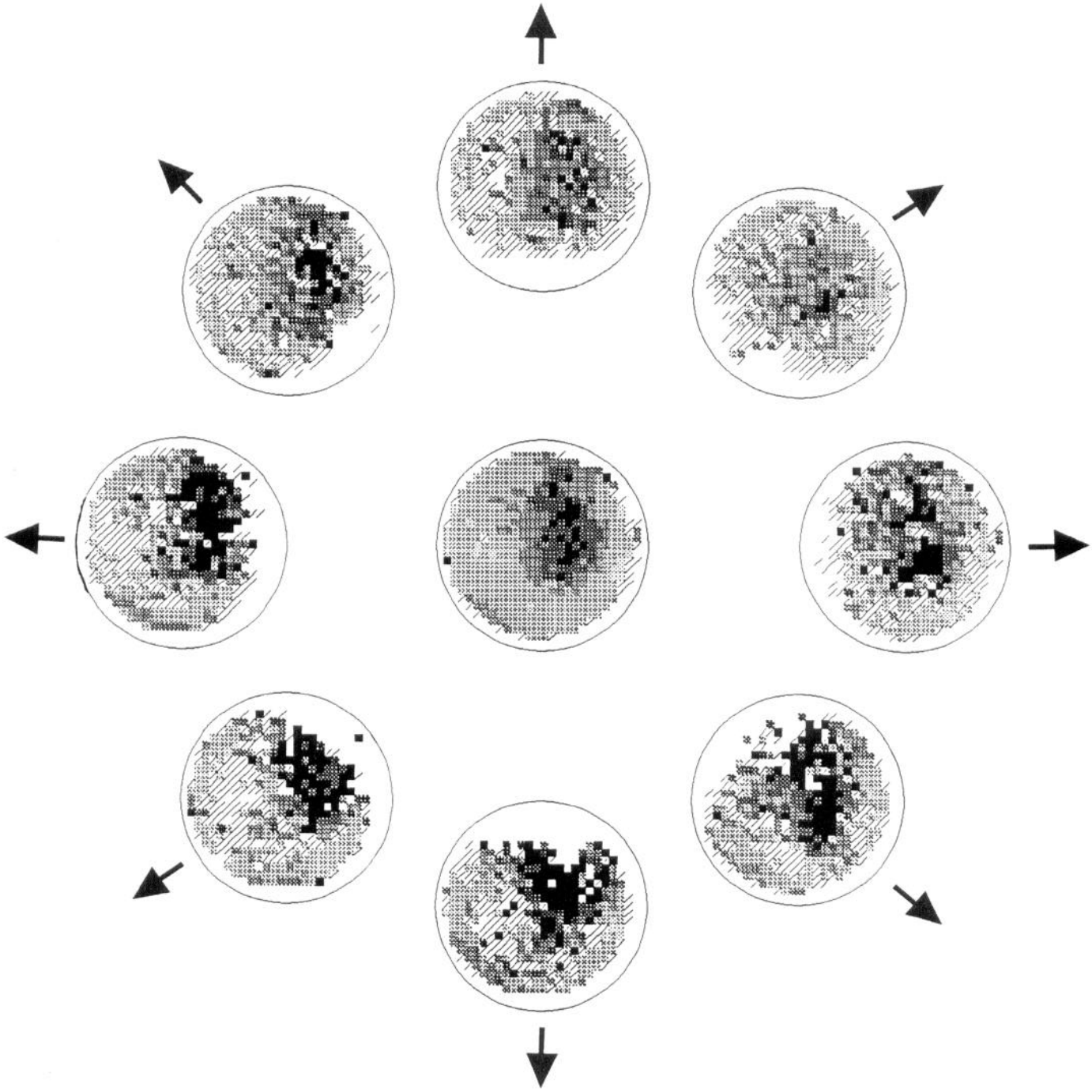

Figure 4. Influence of head direction on firing rate. The *central map* is a standard firing rate map (constructed as in Fig. 2) for a cell whose rate was relatively strongly influenced by directional heading ($\omega^2 = 0.07$). The *surrounding circular array of maps* show the same data separated into bins according to the head direction at the time each data point was sampled. Thus, each surrounding map is constructed from only that portion of the data that was collected when the animal was facing the direction indicated by the accompanying *arrow*. The gray scale values for the circular array maps were selected based on the mean and SD for pixels in the central map. Thus, all maps depict rate using the same scale. This cell showed higher rates for directions indicated in the *lower portions of the circular array*.

showed significant differences for each of the spatial coherence ($df = 84$, $t = 4.46$, $p < 0.001$), rate in nonzero pixels ($df = 84$, $t = 2.13$, $p < 0.05$) and field size ($df = 84$, $t = 2.94$, $p < 0.01$) measures.

There are several possible reasons for the discrepancies between the two methods of statistical analysis (use of hemisphere means versus individual cells as data points). One is that, as mentioned above, collection of a large number of cells from one electrode track constitutes a sampling bias that could result in misrepresentation of true regional averages, for example, as would happen if a large number of cells were recorded from a proximal location in an animal that generally had low values on a particular measure for cells throughout its subiculum. Another possibility is that the reduction in N involved in going from indi-

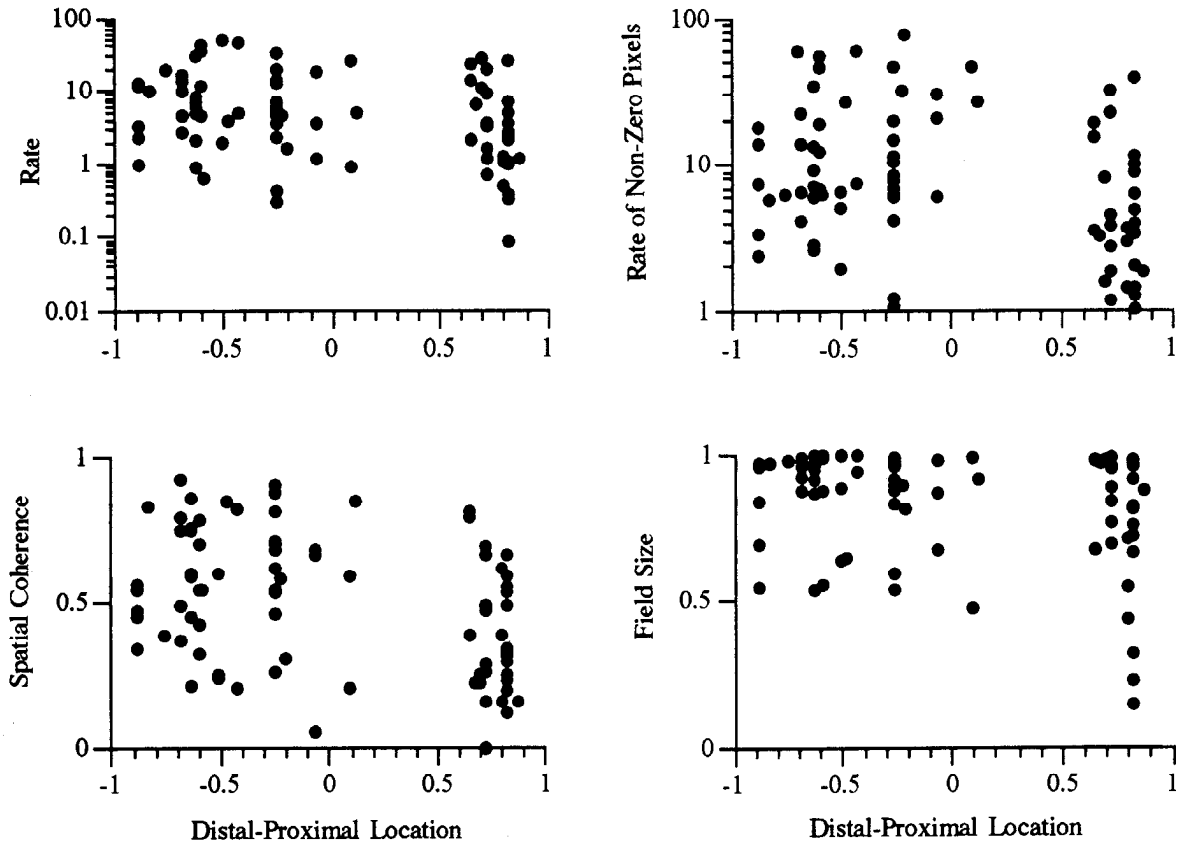

Figure 5. Firing properties of individual cells as a function of transverse location within the subiculum. The firing rate, average rate in nonzero pixels, spatial coherence, and field size for individual cells are shown as a function of anatomical location. (Note log scale for the two rate measures.) Anatomical location is indicated on the *abscissa* along a scale in which locations from the middle of the subiculum to the proximal edge range from 0.0 to 1.0 while those from the middle to the distal edge range from 0.0 to −1.0. Note that cells recorded from the same electrode appear along the same vertical location. Average values for each measure are slightly lower for cells in the proximal region.

vidual cells to hemispheric means, could make small, but genuine, differences between the distal and proximal areas undetectable. Another factor has to do with the possibility that there is large variability on these measures within very local regions of the subiculum. Such variability would make it so that the true mean value for the cells along a single electrode track could be very poorly estimated in cases in which just one or two cells were collected along that track. Such cases would contribute disproportionately to estimates of the mean and variance when these are calculated based on hemisphere means.

This list of differences between the two approaches to the statistical tests makes it clear that there are advantages and disadvantages to both methods. To attempt to gain insight into whether real differences between the proximal and distal subicular regions exist, the individual cell data points for each measure were displayed as a function of location along the transverse axis of the subiculum (Fig. 5). For this, transverse location was indicated on a scale in which the middle of the subiculum was assigned the value of zero, while locations proximal to this ranged from 0.0 to 1.0, and locations distal to this ranged from 0.0 to −1.0. The electrode track for each cell was located along this scale, and the values of each of the rate, rate of nonzero pixels, spatial coherence, and field size measures for each cell along that track were plotted in Figure 5. From this it can be seen, first, that there is much overlap in points from the two regions. Second, there is also, as speculated, large variability between the cells recorded along a single electrode track (located in Fig. 5 along a single vertical strip). Third, there are not cases in which a large number of cells were collected from a single electrode track in which the cells were aberrant in relation to those from other tracks in the same general area (with the possible exception of the field size measure, in which two cells contributed some unusually low values). Taken together, these observations make it seem that taking the individual cell data for use in statistical analysis may be the more appropriate approach in this case. This, along with the overall pattern of differences between the two regions observable in Figure 5, makes it seem that there probably are small but reliable differences between the proximal and distal regions in each of rate of nonzero pixels, spatial coherence, and field size measures.

The fact that both spatial coherence and firing rate were higher in the distal region of subiculum allows for the possibility that these two variables were related, such that factors leading to higher rates also lead to higher spatial coherence for individual cells. In addition, the interpretation of differences in spatial coherence between the two subicular regions is confounded by differences in rate, since it is possible that higher firing rates could lead to better sampling of the true rate of firing in a given pixel. This may, in turn, artifactually lead to higher values for spatial coherence. As a general test of the relationship between these two variables, a correlation coefficient was calculated for rate and spatial coherence values of the cells within each region. These coefficients were small and insignificant in each of the distal (df = 51, $R = -0.19$) and proximal (df = 34, $R = 0.08$)

Table 2. Averages of firing property measures for cells grouped according to cell type

Measure	Bursters	Nonbursters	Depolarized bursters	Theta cells
Overall rate	3.91 (±0.71)	4.08 (±0.72)	13.73 (±1.82)	37.32 (±2.81)
Mean rate for nonzero pixels	5.64 (±0.91)	6.46 (±0.93)	21.98 (±3.07)	51.28 (±4.54)
Spatial coherence	0.44 (±0.04)	0.46 (±0.04)	0.62 (±0.07)	0.48 (±0.06)
Field size	0.70 (±0.04)	0.79 (±0.04)	0.97 (±0.01)	0.99 (±0.003)
N	29	35	12	10

Values are given as means (±SE).

regions. Note that the correlation is actually negative in the distal region. This suggests that differences in spatial coherence do not result artifactually from differences in rate, and that at least some influences on the two variables are independent.

Cell types based on spike train patterns

Examination of the interspike interval and autocorrelation histograms for each cell revealed that most cells could be classified into one of four types. Figure 6 shows an example of the interspike interval histogram (upper histogram of each pair) and autocorrelation histogram (lower histogram of each pair) for a representative cell from each group.

One cell type showed a large, single, early (between 2 and 4 msec) peak in the interspike interval histogram. This early peak accounted for the majority of interspike intervals in the record. This pattern suggested a strong tendency to fire in bursts, with interspike intervals of 2–4 msec. Because of this, these cells have been labeled "bursters," and are tentatively identified as corresponding to the bursting cells identified *in vitro* by Stewart and Wong (1993). Bursting cells tend to have a low firing rate, and their autocorrelation usually shows some evidence of modulation within the frequency range of the theta EEG pattern (5–12 Hz), which can be observed in the hippocampal formation.

A second cell type had virtually no firing in the 2–4 msec interspike interval bins but, instead, showed a later peak between 7 and 25 msec. These cells have been labeled "nonbursters," and may correspond to the nonbursting cells identified by Stewart and Wong (1993). They also tend to have a low firing rate, but show less evidence of theta modulation than do the bursting cells.

A third type of cell showed both an early and a late peak in the interspike interval histogram. The early peak occurred between 1 and 2 msec, while the later peak was at 20–40 msec. It is possible that this kind of pattern resulted from the oscillation of bursting cells between a bursting and nonbursting mode, as described by Stewart and Wong (1993). As mentioned in the introductory remarks, these workers found that bursting cells could be made to enter a nonbursting mode as a result of depolarization of the cell membrane. Thus, the early peak could result from spikes that occur when the cell is at normal levels of polarization, while the second peak could result during a nonbursting mode caused by depolarization. Compatible with this suggestion is the fact that these cells have a relatively high firing rate, suggesting that they may be tonically excited (and, thus, depolarized) under the conditions of the recording session. These cells have been tentatively labeled "depolarized bursters."

The last cell type appeared similar to a type known as "theta cells" that have been identified in the hippocampus (Ranck, 1973). Like hippocampal theta cells, these cells showed high firing rates, short spike width (mean = 210.62 μsec), and rates that were strongly modulated within the frequency range of the theta EEG pattern. It was not clear whether the cells studied here showed the same behavioral correlates as hippocampal theta cells (increased firing during locomotor activity), since the animals in this study showed continuous, homogeneous locomotor behavior. These cells showed no interspike interval peak in the 2–4 msec range; instead, there was a single, later peak between 7 and 15 msec.

Finally, 13 cells could not be clearly placed into any of these categories.

To examine the relationship between these types of spike train patterns and other firing properties, the mean values for overall rate, mean rate of nonzero pixels, spatial coherence, and field size were calculated for the cells in each of these categories (Table 2). The bursters and nonbursters showed similar values for all these measures, while the depolarized bursters showed higher values overall. The field size for the depolarized bursters was 97%, indicating that they fired throughout almost all of the cylinder, and this is compatible with the suggestion (above) that these cells were tonically depolarized in this situation. Theta cells showed the highest rates and field size of all groups, but showed spatial coherence values comparable to those of the bursters and nonbursters.

→

Figure 6. Interspike interval and autocorrelation histograms for a representative example of one cell from each of the cell types. Interspike interval histograms (*upper histogram of each pair*) were constructed by summing the number of occurrences of intervals (between successive spikes for the cell under study) that fell within each 1 msec time bin from 0 to 300. (Note that the 0–1 msec bin must always be empty, due to the refractory period of the cell.) The sum of each bin was then divided by the total number of interspike intervals, in order to obtain the proportion of interspike intervals that fell within each 1 msec time range. Any tendency for a cell to fire in bursts at a given frequency will show up as a peak at the corresponding interval in the interspike interval histogram. Autocorrelation histograms (*lower histogram of each pair*) were constructed by summing the number of times in which a spike occurred within each 1 msec bin from 0 to 300, given the occurrence of a spike at time 0. These sums were then divided by the total time, to yield the rate of occurrence for each interval. These histograms reveal any rhythmic modulation of cell rate, and also provide an indication (based on the average height of the histogram bars) of the overall firing rate. Note the different scale necessary for the theta cell autocorrelation, due to the high firing rate of this type of cell.

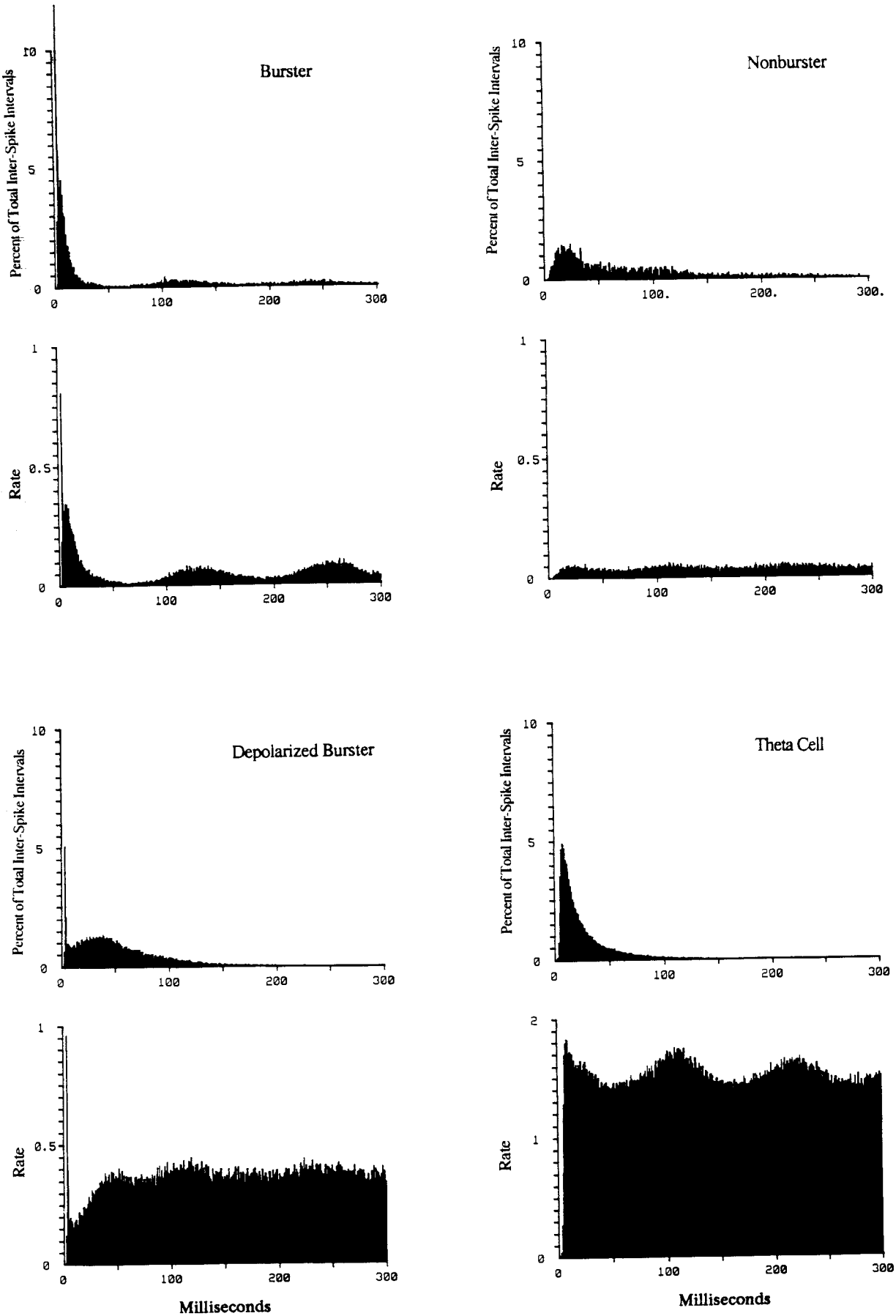
Burster
Percent of Total Inter-Spike Intervals
Rate
Nonburster
Depolarized Burster
Theta Cell
Milliseconds

Table 3. Averages of firing property measures for cells grouped according to anatomical location and cell type

Measure	Distal subiculum	Proximal subiculum	Hippocampo subicular border
Bursters			
Overall rate	4.54 (±1.16)	3.19 (±0.96)	4.43 (±1.93)
Mean rate for nonzero pixels	7.11 (±1.66)	5.05 (±1.20)	5.69 (±2.12)
Spatial coherence	0.63 (±0.07)	0.39 (±0.04)	0.32 (±0.09)
Field size	0.80 (±0.05)	0.69 (±0.05)	0.61 (±0.14)
N	9	13	7
Nonbursters			
Overall rate	4.57 (±0.79)	3.44 (±1.82)	3.35 (±1.77)
Mean rate for nonzero pixels	7.69 (±1.10)	4.84 (±2.09)	4.59 (±2.44)
Spatial coherence	0.55 (±0.05)	0.34 (±0.07)	0.21 (±0.09)
Field size	0.83 (±0.03)	0.72 (±0.09)	0.75 (±0.12)
N	20	10	4
Depolarized bursters			
Overall rate	13.59 (±1.51)	19.70 (±5.83)	–
Mean rate for nonzero pixels	19.81 (±2.50)	32.79 (±14.14)	–
Spatial coherence	0.64 (±0.06)	0.50 (±0.30)	–
Field size	0.97 (±0.01)	0.98 (±0.005)	–
N	10	2	0
Theta cells			
Overall rate	39.17 (±3.07)	26.64 (±0.63)	45.80
Mean rate for nonzero pixels	53.60 (±4.92)	34.98 (±4.11)	67.05
Spatial coherence	0.48 (±0.09)	0.40 (±0.15)	0.58
Field size	0.99 (±0.004)	0.98 (±0.005)	0.99
N	7	2	1

Values are given as means (±SE).

For the purpose of statistical analysis, mean values were obtained for cells of each type for each electrode track. Analysis of the effect of cell type on overall rate yielded a highly significant F value of 87.44 (df = 41,3, $p < 0.001$). A Tukey test (Keppel, 1973) for pairwise comparisons between means showed that theta cells had higher rates than all other groups (at the 0.05 level), while depolarized bursters were also significantly different from all other groups. Bursters and nonbursters were not significantly different from each other on this measure. Analysis of rate for nonzero pixels yielded a very similar set of results, with an F value of 65.41 (df = 41,3, $p < 0.001$), and identical outcomes for pairwise comparisons between means. Analysis of differences in field size were also highly significant (df = 41,3, $F = 11.25$, $p < 0.001$), and comparisons between means showed that both the bursters and nonbursters were significantly different from both the depolarized bursters and theta cells. In addition, bursters and nonbursters were significantly different from each other. The analysis for the effect of cell type on spatial coherence only approached significance (df = 41,3, $F = 1.71$, $p < 0.25$).

Finally, it should be noted that bursters and nonbursters were found in roughly equal numbers, while the depolarized bursters and theta cells were relatively few in number. If the burster and depolarized burster cells are counted together (assuming that they both come from the same pool of cells whose basic physiological properties are homogeneous) then the ratio of total bursting to nonbursting cells is 41:35. This is somewhat smaller than the ratio of 49:23 found by Stewart and Wong (1993).

Summary of firing properties for cell types within each subicular region

Table 3 provides summary data for each of the cell types grouped according to anatomical region within the subiculum. The overall pattern of differences in the rate measures, spatial coherence, and field size between the proximal and distal regions of subiculum is maintained within each of the burster, nonburster, and theta cell categories.

Also notable is the fact that 10 of 12 of the depolarized bursters were found in the distal region. In addition, examination of the histological data showed that the two depolarized bursters categorized here as being in the proximal region were both very close to the proximo-distal border, suggesting that they may have been miscategorized in terms of their anatomical location. This regional difference in the location of depolarized bursters, along with regional differences in rate, suggests that cells in the distal region of subiculum receive higher levels of tonic excitation, which causes some of the bursting cells to enter a depolarized, nonbursting mode, and also causes generally higher rates for other cells in this region.

Also, note that the apparently higher spatial coherence value for depolarized bursters (Table 2) is not as apparent when these values are compared with bursters and nonbursters located in the *distal* region. Thus, the apparently higher value seen in Table 2 seems to be related to the fact that depolarized bursters were found mostly in the distal region, where spatial coherence values were otherwise high.

Comparison of firing properties of adjacent cells

The columnar, or slab-like projection pattern of cells from the hippocampus to the subiculum suggested the possibility that firing properties in the subiculum would show a columnar, or slab-like organization, such that cells recorded along the same vertical track would show similar location-related patterns. As one test for this, the firing rate maps for pairs of cells recorded during the same session from the same electrode wire were examined. Four examples of this were available, and two of these are shown in Figure 7. It can be seen that the maps from the two members of each pair do not appear similar to each other.

As a quantitative test for this similarity, pixel-by-pixel correlations were conducted for each pair of maps from simultaneously recorded cells. The average of these correlations was 0.06, range −0.27 to 0.37.

As another test for columnar organization, correlations were conducted for pairs of cells recorded on the same wire of the same electrode (but not during the same session). A total of 37 such pairwise comparisons were available, and the average correlation values for these pairs was 0.0003, range −0.20 to 0.22. Thus, there was no suggestion that cells located along the same vertical strip of subiculum had related spatial patterns.

Environmental manipulations

Figure 8 shows examples of three cells recorded in the set of environmental manipulations described in Materials and Methods. The first map for each cell shows the data from the initial standard recording session (note that the data from this session are missing for one of these cells). The next map shows data from a second session, in which both the entry location and cue card were rotated prior to bringing the animal into the recording session. As can be seen, each cell rotated its firing field along with the card and entry location, suggesting that one or both of these cues were dominant for determining the orientation of the firing pattern. The third map shows results from the session after the animal was transferred directly from the rotated cylinder to the rectangle. Each cell tended to show a robust, location-related firing pattern in the rectangle. Thus, each cell fired throughout much of the area of both the cylinder and the rectangle, and showed a location-related pattern in both. Interestingly, in some cases (the upper two cases shown here) the pattern in the rectangle was similar to that observed in the cylinder, and was even oriented in the same way (in relation to the larger, laboratory framework), in spite of the fact that the cue card was in a different relative angular location in the two environments. No attempt was made to assess this similarity quantitatively; however, of the eight cells tested in this series of manipulations, five appeared to show this replication of field as assessed by visual inspection. The last map for each cell shows results from the session in which the rat was transferred directly from the rectangle into the cylinder after the cylinder had been rotated back to the standard position. Here, each cell rotated back to its standard configuration, suggesting that the cue card, possibly in conjunction with uncontrolled background cues, was the dominant influence for firing pattern orientation. All but one of the cells tested showed this rotation back to the standard orientation.

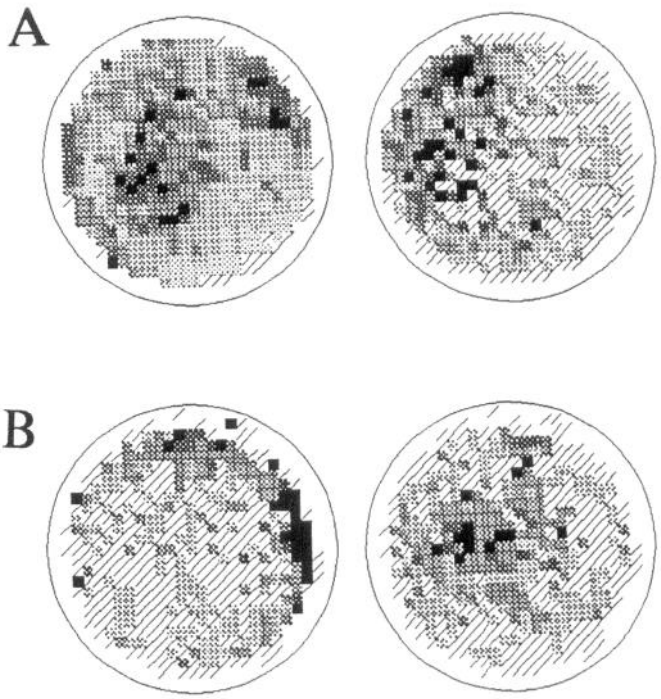

Figure 7. Firing rate maps (constructed as in Fig. 2) for two pairs (*A* and *B*) of cells recorded from the same electrode during the same session. Even though the cells in each pair must have been very close together, they do not have similar spatial patterns.

Discussion

Cells located throughout the transverse extent of the dorsal subiculum showed location-related firing patterns, such that most cells showed a repeatable, statistically significant relationship between spatial location and firing rate. There was considerable variation between cells in the strength of this spatial signal, as assessed by the spatial coherence measure. For the most highly spatial cells, as much as 80% or more of the total pixel-to-pixel variance could be explained by spatial location. Other cells showed little or no spatial modulation, while most cells were located along a continuum between these extremes.

The recording paradigm used here (Muller et al., 1987) was one in which the animals showed constant locomotor behavior that was quite homogeneously distributed both spatially throughout the apparatus, as well as temporally throughout the session time. In addition, the food reward was also homogeneously distributed both temporally and spatially. Thus, this situation provides a useful environment for detection of a spatial signal that is reasonably unconfounded by any effects that might be caused by regionally distributed differences in behavior patterns or the presence of rewarding stimuli. In this way, the pellet-searching paradigm makes it unlikely that the observed spatial patterns were artifactually generated due to the cells having a behavioral correlate other than spatial location, which was non-homogeneously distributed in space.

In fact, one disadvantage of this paradigm is that it largely precludes the detection of most firing correlates other than spatial location. Thus, although not examined here, it seems likely that the subicular cells, if studied in a different situation, might show additional behavioral and contextual correlates, as have been observed for hippocampal cells (see Eichenbaum and Otto, 1993, for review).

The location-related signal seen here was not unexpected, given the massive hippocampal projection to the subiculum. Thus, it seems likely that the patterns observed here were driven

1. Standard Cylinder

2. Rotated Cylinder with Rectangle Present

3. Rectangle with Cylinder Present

4. Cylinder with Rectangle Present

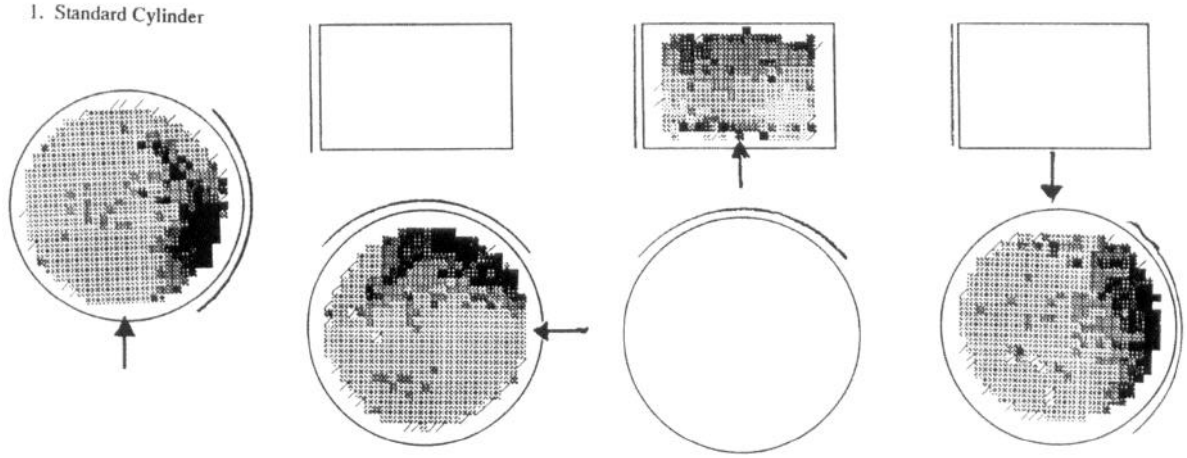

1. Standard Cylinder

2. Rotated Cylinder with Rectangle Present

3. Rectangle with Cylinder Present

4. Cylinder with Rectangle Present

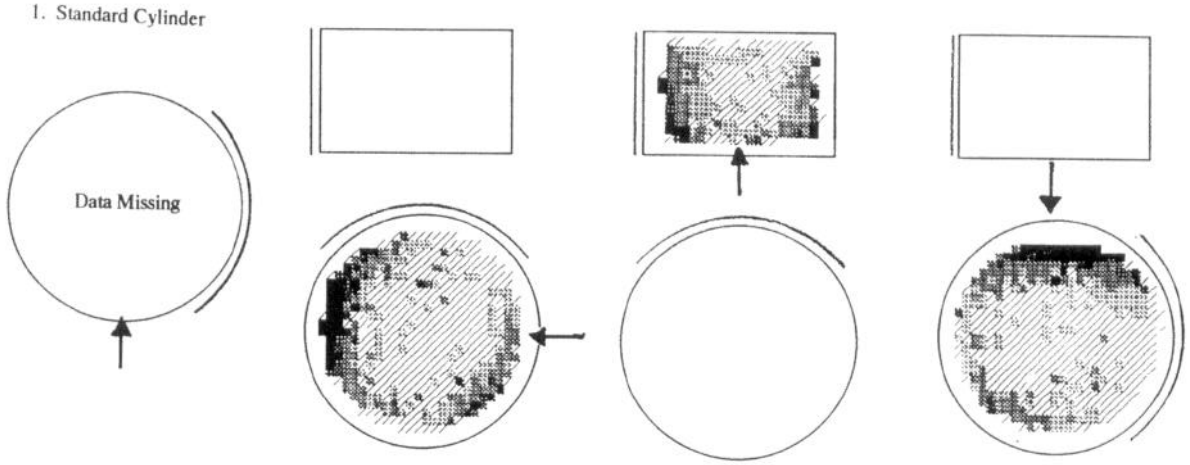

1. Standard Cylinder

2. Rotated Cylinder with Rectangle Present

3. Rectangle with Cylinder Present

4. Cylinder with Rectangle Present

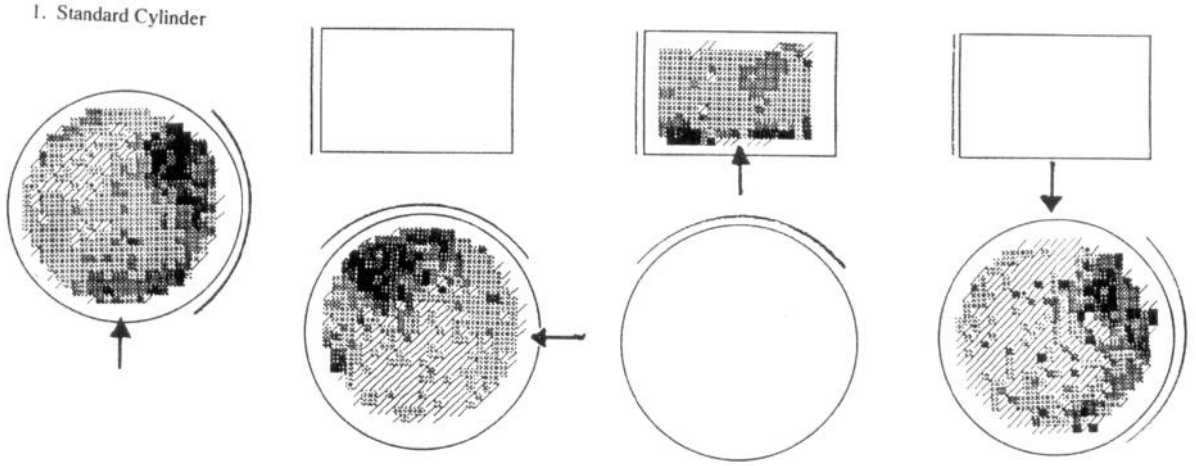

largely by excitatory inputs from hippocampal place cells, as has been suggested elsewhere (Barnes et al., 1990). The subicular firing fields were quite different from those found in the hippocampus, however, in that they were much larger, and they often contained more than one region of high firing, such that they tended to cover much of the floor of the apparatus with a continuous, spatially graded, firing rate pattern. This suggests the possibility that the pattern for any one subicular cell is caused by convergent activity from a number of hippocampal place cells, each with a field in a somewhat different portion of the environment. Indeed, visual inspection of the subicular firing rate maps sometimes revealed localized "hot spots" that roughly corresponded in size and shape to hippocampal place fields (see Fig. 2).

The average spatial coherence value for the subicular cells was 0.48, which is considerably lower than the average of 0.80 obtained in the same recording apparatus for hippocampal place cells (reported in Kubie et al., 1990). This suggests that the strength of the subicular spatial signal may be less than that found in the hippocampus. There were, however, at least some subicular cells (11%) whose spatial coherence value was at or above the hippocampal complex spike cell average. In addition, there were differences between the two studies in the manner in which the cell populations were sampled. Here, every cell that could be electrically isolated was included in the data set, regardless of whether it appeared to have a spatial component to its firing pattern. In contrast, the data reported by Kubie et al. (1990) were taken only from hippocampal cells that appeared, by inspection during screening, to have a place field. Thus, it is possible that a subset of cells that were low in spatial coherence was systematically omitted.

These results are similar to those obtained for subicular cells recorded while animals performed on an eight-arm maze (Barnes et al., 1990). That work also reported a highly distributed, but reliable, spatial signal. One apparent difference between the two studies is that Barnes et al. (1990) reported negligible values for subicular cells on the spatial selectivity score used in that study to measure the strength of the spatial signal. However, as the authors point out, that particular measure leads to low values whenever a spatial signal is highly distributed over the maze arms. Thus, it is possible that a metric more similar to the spatial coherence measure used here could have yielded a similar view of the strength of the spatial signal for the subicular cells in that study.

In addition to the location-related rate modulation observed here, many subicular cells also showed a statistically reliable, but small, directional modulation of firing rate. It seems possible that this small directional component may be transmitted from the hippocampus, although it could also be generated by the robust directional signal present in the postsubiculum or related areas (Taube et al., 1990a; see introductory remarks).

Regional variation in firing properties

As mentioned in the introductory remarks, recent anatomical data have shown that the proximal and distal regions of the subiculum have different projection sites (Witter et al., 1990). This raised the question of whether the two halves would also have different behavioral correlates, thus sending a different message to each set of areas. In general, the qualitative aspects of cell activity were quite similar across the two areas. There were, however, some quantitative differences.

Each of the spatial coherence, field size, rate-in-nonzero-pixels, and overall rate measures showed higher average values for cells in the distal, as compared to the proximal portion of the transverse axis of the subiculum. These differences were statistically significant for the first three measures, but only when assessed using the data from each individual cell (rather than hemisphere means) as entries in the analysis. Visual inspection of the overall data pattern (Fig. 5), along with certain statistical considerations (see Results), makes it seem likely that these data reflect genuine differences in the characteristics of cells in these two areas. Additional support for this conclusion comes from data collected from cells in the border region. These cells show values for each measure that are more similar to cells in the proximal, rather than distal, subiculum. It is not clear whether these cells should be included as part of the subicular population; however, if they were included, they would strengthen the claim that there are genuine differences between the proximal and distal regions.

The fact that both field size and rate were higher in the distal region, along with the fact that most of the putative depolarized bursters were found there, suggests that these cells receive a higher level of tonic excitatory input in this recording situation. This idea is strengthened by the fact that these differences were maintained for average values within each of the burster and nonburster categories. Thus, it seems that the rate differences do not result from a differential distribution of cell types across the transverse axis; rather, this pattern suggests that the cells of each type are more strongly driven in the distal region.

The fact that spatial coherence and rate values were both higher in the distal region suggested the possibility that these two variables could be causally related. Thus, for example, it could be that cells in the distal region receive more excitatory input from the hippocampal cells, which causes both higher rates and higher spatial coherence. One piece of evidence that does not support this idea, however, is that the correlation coefficient between rate and spatial coherence for cells within each of the proximal and distal regions was close to zero, and was even negative (−0.19) in the distal region.

It is interesting to speculate on what could be responsible for the differences observed between the distal and proximal regions. Given the topographically organized projections from the hippocampus to the subiculum (Amaral et al., 1991), it is interesting to speculate on whether the differences observed here could reflect differences in place cell properties along the transverse axis of the hippocampus. As far as we are aware, no systematic study relevant to this issue has been conducted. Another possibility is that there are differences in the details of hippocampo-subicular synaptic connectivity across this axis, which could in some way explain these differences.

←

Figure 8. Firing rate maps (constructed as in Fig. 2) for three representative cells that were each recorded during the series of environmental manipulations described in Materials and Methods. *Arrows* indicate the location at which the animal was introduced into the apparatus at the start of each session. *Lines* along the outer edge of the apparatus indicate the orientation of the white cue card that was placed on the inner wall. Note that in all cases, the location-related firing pattern in the cylinder maintained a constant spatial relationship to the cue card, suggesting that this is a dominant cue for determining firing field orientation. For the upper two cells, the location-related pattern in the rectangle was similar to that in the rotated cylinder from which the animal had just been transferred.

One important question about this pattern of proximodistal differences is what, if any, functional consequences they may have for information processing in the regions to which these cells project. Thus, for example, it could be that the slightly lower overall rates observed in proximal subiculum somehow lead to more efficient signal transmission in that set of areas to which it projects. In general, however, the fact that the observed differences are quantitative, rather than qualitative, and are small in magnitude, suggests that any functional consequences of these differences might be quite subtle.

Finally, it should be noted that a different behavioral paradigm (allowing for examination of other possible types of behavioral correlate) could possibly reveal qualitative differences not detected here.

Cell types based on spike train patterns

As reported elsewhere (Barnes et al., 1990), examination of spike train patterns from the subicular cells revealed that there is more diversity in the subicular cell population than has been reported for the hippocampus. Here, the different patterns have been tentatively identified as corresponding to the bursting, nonbursting, and interneuron types identified *in vitro* by Stewart and Wong (1993). In addition, a bimodal type of pattern was observed that was interpreted as possibly resulting from the oscillation of bursting cells between a bursting and nonbursting mode (Stewart and Wong, 1993).

Thus, the presence of a large peak in the 2–4 msec range of the interspike interval histogram suggests the presence of a cell type with intrinsic properties that lead to the generation of a bursting pattern in response to depolarization. Conversely, the absence of such a peak suggests a different set of underlying membrane properties. Whether the burster and nonburster types seen here actually correspond to the types identified by Stewart and Wong (1993) cannot be determined definitively, since intracellular recordings were not possible in this *in vivo* situation. Thus, in the absence of any examination of intrinsic membrane properties, it is possible that the spike train patterns observed here were imposed by the circuit properties of the network in which these cells were embedded. However, the fact that bursting and nonbursting patterns were observed here suggests that membrane properties responsible for these two patterns *in vitro* are also causally involved in similar patterns observed *in vivo* in the freely behaving animal. If true, this strengthens the claim that these intrinsic differences may have functional consequences for information processing under natural circumstances.

Given this consideration, it is interesting that the spatial patterns of the bursting and nonbursting cells were not detectably different from each other on either the rate or spatial coherence measures (although there was a small, significant difference in field size). This suggests that the different intrinsic properties do not, in themselves, necessarily lead to different global patterns for coding environmentally related inputs.

As mentioned in the introductory remarks, it has been observed that cells within any one local region of the subiculum are specialized in terms of their efferent projections, such that two adjacent cells may send afferent projections to different places (Swanson et al., 1981; Donovan and Wyss, 1983). This raises the interesting possibility that differences in projection areas are related to the different cell types, such that some of the projection zones for subicular cells receive inputs from only bursting cells while others receive inputs from nonbursting cells. [It should be noted that Stewart and Wong (1993) reported that both bursting and nonbursting cells could be antidromically from the alveus, suggesting that both are projection neurons.]

It is not clear what the functional consequences of the bursting and nonbursting patterns could be for the areas receiving subicular inputs. One possibility, suggested by the Stewart and Wong (1993) data, is that the bursting cells could be preferentially involved in transmitting rhythmic oscillations (like those at the theta frequency) to other areas, thus entraining these areas to the hippocampal frequency. This possibility is supported by the fact that bursting cells in the present data set showed more evidence of theta-frequency modulation than did nonbursters. It is not clear what the functional consequences could be for the postulated theta-frequency transmission, although activity at this frequency has been shown to be particularly efficacious for inducing LTP (Larson et al., 1986).

Lack of columnar organization

Despite the fact that there is a topographically organized (Amaral et al., 1991), columnar (Tamamaki et al., 1987; Tamamaki and Nojyo, 1990) projection of the hippocampal CA1 cells onto the subiculum, there was no evidence of similarity in the spatial firing patterns of subicular cells along the same vertical trajectory. This suggests that, although a particular set of hippocampal cells may all make dense terminal arborizations within the same local region of subiculum, there is still sufficient variability in which exact hippocampal cells make synaptic contact with a given subicular cell, such that any two adjacent cells receive quite different patterns of spatial input.

Environmental manipulations

The environmental manipulations conducted here revealed, first, that the white card was an important determinant of firing pattern orientation. The firing pattern of each cell (with only one exception during one session) maintained a constant spatial relation to this cue over the course of the card rotation sessions. This was not unexpected, since this cue is also known to be important for the orientation of place fields in hippocampal cells (Muller and Kubie, 1987). Thus, these data are compatible with the suggestion that the subicular patterns are driven by hippocampal inputs.

Sessions in the rectangle revealed that each of the tested cells showed a location-related pattern in this structure as well. In addition, for most of the cells this pattern appeared to be a replica of that in the cylinder. These results are, in some respects, quite different from those for hippocampal place cells. The hippocampal work has shown no detectable relationship between firing patterns of a cell when tested in two different apparati, and in fact, cells that have a field in one environment often show no activity at all in a separate environment (Kubie and Ranck, 1984; Muller and Kubie, 1987; Thompson and Best, 1989).

Thus, the observations here suggest an important difference between hippocampal and subicular cells, and suggest the possibility that subicular cells have a unique ability to transfer an overall abstract spatial representation from one environment to another. These data also suggest that the explanation of subicular cell firing resulting simply from the convergent input of hippocampal place cells is not sufficient, since hippocampal cells tested under similar conditions do not show the same pattern of results (Muller and Kubie, 1987). However, at least one important methodological difference existed between the hippo-

campal study and the work presented here. In the hippocampal work, animals were not transferred directly from one experimental apparatus to the next; rather, they always had an interim period spent in the home cage between each session. It could be that direct transfer of animals from one environment to another would lead to replication of spatial patterns for hippocampal cells as well. This would be an interesting finding, and would suggest that an experience in one environment somehow "sets" the cell to reproduce its present pattern in another, immediately experienced, environment.

Another possible methodological difference could be that, somehow, in this study, sensory differences between the two recording apparati were not as salient as in the hippocampal work (due to a different level of overall illumination, slight differences in the gray paint, etc.). Thus, it could be that the replication of patterns observed here is due to stimulus generalization from the cylinder to the rectangle. Although the rotation manipulations made it clear that the white card was salient in the context of the cylinder, it is possible that it was less so in the rectangle. Indeed, it could be that the geometry of the rectangle caused differential light patterns on each of the four walls, which may have obscured the presence of the card. Thus, the overall similarity of the two environments, along with information that may be available to the system about the rat's overall orientation in relation to the laboratory framework, may have made it such that the various regions of the rectangle were not sufficiently differentiable from corresponding areas of the cylinder.

In summary, the manipulations here suggest the possibility that subicular cells show a robust spatial pattern in many (or even all) possible environments, and may even sometimes show the same overall pattern from one environment to the next. However, further experiments involving sets of environments more dramatically different from each other are necessary to support this suggestion further.

Summary

These results suggest that the dorsal subiculum sends a strong, highly distributed, location-related signal to each of the areas to which it projects. This signal is transmitted via both bursting and nonbursting spike train patterns. It seems likely that the subicular activity is driven largely by hippocampal inputs, and thus, it provides a way that the hippocampal spatial information can reach other brain areas. These areas include structures thought to be involved in a wide variety of learning and memory functions, such as instrumental reward learning (nucleus accumbens), aversive learning (cingulate cortex), and working memory (prefrontal areas). Thus, one role of the subiculum may be to transmit information about the animal's current location in space, so that it may be used for various navigation-related functions, such as route planning, and the storage of information about the spatial location of rewarding and aversive stimuli.

References

Amaral DG, Dolorfo C, Alvarez-Royo P (1991) Organization of CA1 projections to the subiculum: a PHA-L analysis in the rat. Hippocampus 1:415–436.

Andersen P, Bland BH, Dudar JD (1973) Organization of the hippocampal output. Exp Brain Res 17:152–158.

Barnes CA, McNaughton BL, Mizumori SYJ, Leonard BW, Lei-Huey L (1990) Comparison of spatial and temporal characteristics of neuronal activity in sequential stages of hippocampal processing. In: Progress in brain research, Vol 83 (Storm-Mathisen J, Zimmer J, Ottersen OP, eds), pp. 287–299. New York: Elsevier.

Bostock E, Taube J, Muller RU (1988) The effects of head orientation on the firing of hippocampal place cells. Soc Neurosci Abstr 14:127.

Chronister RB, Sikes RW, White LE Jr (1975) Postcommissural fornix: origin and distribution in the rodent. Neurosci Lett 1:199–201.

Donovan MK, Wyss JM (1983) Evidence for some collateralization between cortical and diencephalic efferent axons of the rat subicular cortex. Brain Res 259:181–192.

Eichenbaum H, Otto T (1993) Where perception meets memory: functional coding in the hippocampus. In: Brain mechanisms of perception and memory: from neuron to behavior (Ono T, Squire L, Raichle ME, Perrett DI, Fukuda M, eds), pp 301–329. New York: Oxford UP.

Fibiger HC, Phillips AG (1988) Mesocorticolimbic systems and reward. In: Annals of the New York Academy of Science, Vol 537, The mesocorticolimbic system (Kalivas DW, Nemeroff CB, eds), pp 206–215. New York: NY Academy of Science.

Finch DM, Babb TL (1980) Neurophysiology of the caudally directed hippocampal efferent system in the rat: projections to the subicular complex. Brain Res 197:11–26.

Finch DM, Babb TL (1981) Demonstration of caudally directed hippocampal efferents in the rat by intracellular injection of horseradish peroxidase. Brain Res 214:405–410.

Fox SE, Ranck JB Jr (1975) Localization and anatomical identification of theta and complex spike cells in dorsal hippocampal formation of rats. Exp Neurol 49:299–313.

Gabriel M (1990) Functions of the anterior and posterior cingulate cortex during avoidance learning in rabbits. In: Progress in brain research series, Vol 85, The prefrontal cortex: its structure, function, and pathology (Uylings BM, van Eden CG, De Bruin FPC, Corner MA, Feenstra MGP, eds), pp 467–483. Amsterdam: Elsevier.

Goldman-Rakic PS (1987) Circuitry of primate prefrontal cortex and regulation of behavior by representational memory. In: Handbook of physiology, Sec 1, The nervous system (Mountcastle VB, Plum F, Geiger SR, eds), pp 373–417. Bethesda, MD: American Physiological Society.

Hjorth-Simonsen A (1973) Some intrinsic connections of the hippocampus in the rat: an experimental analysis. J Comp Neurol 147: 145–162.

Keppel G (1973) Design and analysis: a researchers handbook. Englewood Cliffs, NJ: Prentice-Hall.

Kubie JL, Ranck JB Jr (1984) Hippocampal neuronal firing, context, and learning. In: Neuropsychology of memory (Squire LR, Butters N, eds), pp 417–423. New York: Guilford.

Kubie JL, Muller RU, Bostock E (1990) Spatial firing properties of hippocampal theta cells. J Neurosci 10:1110–1123.

Larson J, Wong D, Lynch G (1986) Patterned stimulation at the theta frequency is optimal for the induction of hippocampal long-term potentiation. Brain Res 368:347–350.

McNaughton BL, Barnes CA, O'Keefe J (1983) The contributions of position, direction, and velocity to single unit activity in the hippocampus of freely-moving rats. Exp Brain Res 52:41–49.

Meibach RC, Siegel A (1975) The origin of fornix fibers which project to the mammillary bodies in the rat: a horseradish peroxidase study. Brain Res 88:508–512.

Meibach RC, Siegel A (1977a) Efferent connections of the hippocampal formation in the rat. Brain Res 124:197–224.

Meibach RC, Siegel A (1977b) Thalamic projections of the hippocampal formation: evidence for an alternative pathway involving the internal capsule. Brain Res 134:1–12.

Meibach RC, Siegel A (1977c) Subicular projections to the posterior cingulate cortex in rats. Exp Neurol 57:264–274.

Morris RGM, Garrud P, Rawlins JNP, O'Keefe J (1982) Place navigation impaired in rats with hippocampal lesions. Nature 297:681–683.

Muller RU, Kubie JL (1987) The effects of changes in the environment on the spatial firing of hippocampal complex-spike cells. J Neurosci 7:1951–1968.

Muller RU, Kubie JL, Ranck JB Jr (1987) Spatial firing patterns of hippocampal complex-spike cells in a fixed environment. J Neurosci 7:1935–1950.

O'Keefe J (1976) Place units in the hippocampus of the freely-moving rat. Exp Neurol 51:78–109.

O'Keefe J, Dostrovsky J (1971) The hippocampus as a spatial map. Preliminary evidence from unit activity in the freely moving rat. Brain Res 34:171–175.

O'Keefe J, Nadel L (1978) The hippocampus as a cognitive map. New York: Oxford UP.
O'Keefe J, Nadel L, Keightly S, Kill D (1975) Fornix lesions selectively abolish place learning in the rat. Exp Neurol 48:152–166.
Olton DS, Walker JW, Gage FH (1978) Hippocampal connections and spatial discrimination. Brain Res 139:295–308.
Ranck JB Jr (1973) Studies on single neurons in dorsal hippocampal formation and septum in unrestrained rats. I. Behavioral correlates and firing repertoires. Exp Neurol 41:461–535.
Rosene DL, Van Hoesen GW (1977) Hippocampal efferents reach widespread areas of the cerebral cortex and amygdala in the rhesus monkey. Science 198:315–317.
Schenk F, Morris RGM (1985) Dissociation between components of spatial memory in rats after recovery from the effects of retrohippocampal lesions. Exp Brain Res 58:11–28.
Sorensen KE, Shipley MT (1979) Projections from the subiculum to the deep layers of the ipsilateral presubicular and entorhinal cortices in the guinea pig. J Comp Neurol 188:259–264.
Steward O (1976) Topographic organization of the projections from the entorhinal area to the hippocampal formation of the rat. J Comp Neurol 167:285–314.
Stewart M, Wong RKS (1993) Intrinsic properties and evoked responses of guinea-pig subicular neurons *in vitro*. J Neurophysiol 70: 232–245.
Sutherland RJ, Wishaw IQ, Kolb B (1983) A behavioral analysis of spatial localization following electrolytic kainate- or colchicine-induced damage to the hippocampal formation in the rat. Behav Brain Res 7:133–153.
Suzuki WA, Zola-Morgan S, Squire LR, Amaral DG (1993) Lesions of the perirhinal and parahippocampal cortices in the monkey produce long-lasting memory impairment in the visual and tactual modalities. J Neurosci 13:2430–2451.
Swanson LW, Cowan WM (1975) Hippocampo-hypothalamic connections: origin in subicular cortex, not Ammon's horn. Science 189: 303–304.
Swanson LW, Cowan WM (1977) An autoradiographic study of the organization of the efferent connections of the hippocampal formation in the rat. J Comp Neurol 172:49–84.
Swanson LW, Wyss JM, Cowan WM (1978) An autoradiographic study of the organization of the intrahippocampal association pathways in the rat. J Comp Neurol 181:681–716.
Swanson LW, Sawchenko PE, Cowan MW (1981) Evidence for collateral projections by neurons in Ammon's horn, the dentate gyrus, and the subiculum: a multiple retrograde labeling study in the rat. J Neurosci 5:548–559.
Tamamaki N, Noyjo Y (1990) Disposition of the slab-like modules formed by axon branches originating from single CA1 pyramidal neurons in the rat hippocampus. J Comp Neurol 291:509–519.
Tamamaki N, Abe K, Noyjo Y (1987) Columnar organization in the subiculum formed by axon branches originating from single CA1 pyramidal neurons in the rat hippocampus. Brain Res 412:509–519.
Taube JS, Muller RU, Ranck JB Jr (1990a) Head-direction cells recorded from the postsubiculum in freely moving rats. I. Description and quantitative analysis. J Neurosci 10:420–435.
Taube JS, Muller RU, Ranck JB Jr (1990b) Head-direction cells recorded from the postsubiculum in freely moving rats. II. Effects of environmental manipulations. J Neurosci 10:436–447.
Taube JS, Kesslak JP, Cotman CW (1992) Lesions of the rat postsubiculum impair performance on spatial tasks. Behav Neural Biol 57:131–143.
Thompson LT, Best PJ (1989) Place cells and silent cells in the hippocampus of freely-moving rats. J Neurosci 9:2382–2390.
Van Groen T, Wyss JM (1990) The postsubicular cortex in the rat: characterization of the fourth region of the subicular cortex and its connections. Brain Res 529:165–177.
Witter MP, Ostendorf RH, Groenewegen HJ (1990) Heterogeneity in the dorsal subiculum of the rat: distinct neuronal zones project to different cortical and subcortical targets. Eur J Neurosci 2:718–725.
Zola-Morgan S, Squire LR, Amaral DG, Suzuli WA (1989) Lesions of perirhinal and parahippocampal cortex that spare the amygdala and hippocampal formation produce severe memory impairment. J Neurosci 9:4355–4370.
Zola-Morgan S, Squire LR, Clower RP, Rempel NL (1993) Damage to the perirhinal cortex exacerbates memory impairment following lesions to the hippocampal formation. J Neurosci 13:251–265.